Domain swapping of a llama VHH domain builds a crystal-wide β-sheet structure

Silvia Spinelli[a], Aline Desmyter[a], Leon Frenken[b], Theo Verrips[b,1], Mariella Tegoni[a], Christian Cambillau[a,*]

[a] *Architecture et Fonction des Macromolécules Biologiques, UMR-6098, CNRS and Universités d'Aix-Marseille I and II, 31 Chemin Joseph Aiguier, 13402 Marseille Cedex 20, France*

[b] *Unilever Research Vlaardingen, Olivier van Noortlaan 120, 3133 AT Vlaardingen, The Netherlands*

Received 17 February 2004; revised 12 March 2004; accepted 12 March 2004

First published online 29 March 2004

Edited by Hans Eklund

Abstract Among mammals, camelids have a unique immunological system since they produce functional antibodies devoid of light chains and CH1 domains. To bind antigens, whether they are proteins or haptens, camelids use the single domain VH from their heavy chain (VHH). We report here on such a llama VHH domain (VHH-R9) which was raised against a hapten, the RR6 red dye. This VHH possesses the shortest complementarity determining region 3 (CDR3) among all the known VHH sequences and nevertheless binds RR6 efficiently with a K_d value of 83 nM. However, the crystal structure of VHH-R9 exhibits a striking feature: its CDR3 and its last β-strand (β9) do not follow the immunoglobulin VH domain fold, but instead extend out of the VHH molecular boundary and associate with a symmetry-related molecule. The two monomers thus form a domain-swapped dimer which establishes further contacts with symmetry-related molecules and build a crystal-wide β-sheet structure. The driving force of the dimer formation is probably the strain induced by the short CDR3 together with the cleavage of the first seven residues.

Key words: Crystal structure; Camelid heavy-chain antibody VH domain; Immunoglobulin; Red dye hapten; Domain swapping

1. Introduction

The fundamental molecules dedicated to molecular recognition in the humoral immune response are remarkably homogeneous throughout the vertebrate phylum [1]. Important deviations of this conserved immunoglobulin organization have been observed, however. In some immunoglobulin isotypes of camelids from the old world (camels, dromedaries) or from the new world (llamas, vicuña) the L chain is missing [2]. Furthermore, their H chain is devoid of the CH1 domain [3,4] due to an unconventional splicing event during mRNA maturation. The antigen binding fragment of the heavy-chain antibodies therefore comprises a single domain, referred to as VHH, that replaces a four-domain Fab fragment in the immunoglobulin structure [5]. This VHH domain is obtained after a DNA recombination between dedicated VHH germline gene segments with D and J minigenes.

From a structural viewpoint, the three-dimensional structures of VHH unbound [6,7] or in complex with proteins such as lysozyme, RNase, carbonic anhydrase, amylase [8–11] as well as with two dye haptens [12,13], have been determined. They all present a common architecture of the core, with the characteristic mutations of camelid antibodies [14]. The complementarity determining regions (CDRs) 1 and 2 present a length within the average of classical antibodies, while CDR3 can be much longer than usually observed, presents a large variety of conformations and is often stabilized by a disulfide bridge [14]. VHH-R9 was raised against the red dye hapten RR6, for which it has good affinity. VHH-R9 exhibits the shortest CDR3 among camelid VHHs, to date. Its first β-strand has been cleaved between residues 7 and 8 and lacks the first seven residues. The VHH-R9 crystal structure reveals that CDR3 and the last β-strand are swapped between symmetry-related molecules [15]. The resulting dimer forms a crystal-wide β-sheet, a striking feature which involves mechanisms comparable to those occurring during amyloid fiber formation [15]. These findings could give clues on the phenomena which could occur upon conformational changes of VH domains resulting from the presence of short CDRs and proteolytic cleavage.

2. Materials and methods

2.1. VHH preparation and characterization

A male llama (*Lama glama*) was immunized with a bovine serum albumin (Sigma, A7888)-coupled RR6 azo dye (ICI, Procion Rubine MX-B). Young adult male llamas were injected on days 0, 21 and 35 with 250 mg of the antigens mentioned above in Specol (ID-DLO, Lelystad, The Netherlands). Blood samples of about 150 ml were taken 7 days after the last immunization and peripheral blood cells were obtained via Ficoll (Pharmacia) discontinuous gradient centrifugation. From these cells, total RNA was isolated and synthesis of the first strand cDNA was performed (Amersham first strand cDNA kit). DNA fragments encoding the VHH domain were amplified by polymerase chain reaction using specific primers and were ligated into a *Saccharomyces cerevisiae* expression plasmid. After transformation of *S. cerevisiae*, the culture supernatants of single colonies where tested via enzyme-linked immunosorbent assay for the production of RR6-specific VHH fragments. Several VHHs were obtained at very high

*Corresponding author. Fax: (33)-4-91164536.
E-mail address: cambillau@afmb.cnrs-mrs.fr (C. Cambillau).

[1] Present address: Department of Molecular and Cellular Biology, University of Utrecht, 3500 TB Utrecht, The Netherlands.

Abbreviations: VHH, camelid heavy-chain antibody VH domain; CDR, complementarity determining region; FU, functional unit of domain-swapped dimers

0014-5793/04/$30.00
doi:10.1016/S0014-5793(04)00304-7

Table 1
Data collection, structure determination and refinement summary of VHH-R9

Data collection	R9
Total/unique number of reflections	408 060/12 481
% of data > 1σ (overall/last shell)[a]	98.6/98.6
Overall $I/\sigma(I)$ (last shell)	4.9/2.3
Resolution limits	30.0/1.94
R-merge (%) (overall/last shell)[a]	9.4/27.3
Refinement	
Number of protein/solvent atoms	788/73
Number of reflections	12 041
Resolution limits (Å)	15.0–1.95
R/*R*-free value (%)	20.6/22.5
rmsd on bonds (Å) and angles (°)	0.013/1.7
Mean *B* factor (Å^2): main-chain atoms	
main chain atoms	21.5
side chain atoms/solvent	24.0/29.0

[a]Last shell: 2.1–1.94 Å.

yields (up to 100 mg/l of flask culture). The R9 anti-RR6 fragment was purified from crude yeast culture broth by affinity chromatography, using a protein A-Sepharose FF column (Pharmacia). More details on the VHH production procedure have been published elsewhere [16].

Kinetic measurements were performed using an IAsys Biosensor Instrument (Fisons) in phosphate-buffered saline (10 mM Na_2HPO_4, 1 mM KH_2PO_4, 137 mM NaCl, pH 7.4) with 0.05% (v/v) Tween 20, pH 7.4. RR6 was linked to aminosilane cuvettes. At least 10 dilutions were injected into the cuvette. The resulting data were analyzed using the FASTFIT software considering the association phase resulting in association and dissociation constants.

Mass analysis of recombinant VHH-R9 was obtained with Voyager-DE RP (PerSeptive Biosystems). Samples (0.7 μl containing 15 pmol) were mixed with an equal volume of sinapinic acid matrix solution and spotted on the target, then dried at room temperature for 10 min. The mass standard was apomyoglobin.

2.2. Crystallization, data collection and processing

Trials of crystallizations using Crystal Screen (Hampton Research) were carried out at room temperature using the hanging drop method. Crystals suitable for X-ray measurement were obtained at pH 7.5 with the reservoir solution containing 26–28% (v/v) PEG 600 and 100 mM HEPES buffer. An equi-amount of reservoir solution was added to 2 μl of VHH-R9 (20 mg/ml), and the sample solution was equilibrated over 1.0 ml reservoir solution. Crystals of dimensions $0.2\times0.2\times0.1$ mm appeared in 4–5 weeks. VHH-R9 crystallized in the cubic space group $I4_132$ with unit cell dimensions of $a=b=c=124.3$ Å. They contain one VHH-R9 molecule per asymmetric unit giving a V_m value of 3.5 Å^3/Da [17]. It should be noticed that all attempts to crystallize VHH-R9 in complex with its hapten failed.

Crystals were frozen at 100 K without cryoprotectant. One flash-frozen crystal was used for data collection on ID14EH2 (ESRF, Grenoble, France). Data were indexed and integrated with DENZO [18] and scaled using SCALA [19]. The statistics of the data sets are shown in Table 1.

2.3. Structure determination and refinement

The crystal structure was solved using molecular replacement with the AMoRe program [20] in the resolution range 7.0–2.8 Å. The anti-RR6 llama VHH-R2 (PDB: 1QD0) was used as the search model [12]. A unique solution was found with a correlation coefficient of 0.767 and an *R* factor of 33%, compared to the next highest peak with values of 0.375 and 52.0%. Model building was performed using the program Turbo-Frodo [21]. Crystallographic refinement was carried out with the programs CNS [22] and REFMAC [23]. Some 9% of the measured reflections were not included in the refinement procedure and served as a test set, yielding the *R*-free factor. Several rounds of refinement and model building yielded improved maps. The final model was refined to an *R* factor of 20.6% and an *R*-free of 22.5% (Table 1). The stereochemistry of the final model was analyzed by PROCHECK [24], 92.5% of the residues were found to lie in the most favorable regions of the Ramachandran plot and 4.8% in additionally allowed regions, and no residue was found in forbidden regions. The coordinates have been deposited with the Protein Data Bank at RCSB (http://www.rcsb.org/pdb/) as entry 1SJV.

```
          .........!10.......!20.....30!.abc.........!40.....50!..abcdef.....60!..
RR6-R9    QVQLQESGGGLVQAGESLKLSCAASGNTFSG---GFMGWYRQAPGKQRELVATIN------SRGITNYADF
RR6-R2    QVQLQESGGGLVQAGGSLRLSCAASGRATSGHGHYGMGWFRQVPGKEREFVAAIRW-----SGKETWYKDS
RR1-52    QVQLQESGGGLVQAGDSLKLSCEASGDSIGT---YVIGWFRQAPGKERIYLATIGRNLVGPSDFYTRYADS
hCG-H14   QVQLQESGGGLVQAGGSLRLSCAASGRTGST---YDMGWFRQAPGKERESVAAINW-----DSARTYYASS
cAb-LYS3  DVQLQASGGGSVQAGGSLRLSCAASGYTIGP---YCMGWFRQAPGKEREGVAAINM-----GGGITYYADS
cAb-RN05  QVQLVESGGGLVQAGGSLRLSCAASGYAYTY---IYMGWFRQAPGKEREGVAAMDS-----GGGGTLYADS
cAb-CA05  QVQLVESGGGSVQAGGSLRLSCAASGYTVST---YCMGWFRQAPGKEREGVATIL-------GGSTYYGDS
AMYL-B07  QVQLVESGGGSVQAGGSLRLSCAASGYTFSS---YPMGWYRQAPGKECELVSRIF------SDGSANYAGS
AMYL-D09  QVQLVESGGGSVQAGGSLSLSCAASTYTDT------VGWFRQAPGKEREGVAAIYR-----RTGYTYSADS
AMYL-D10  DVQLVESGGGTVPAGGSLRLSCAASGNTLCT---YDMSWYRRAPGKGRDFVSGID------NDGTTTYVDS

          .....70!.......80!..abc.....90!......100!abcdefghijklmnop......110!...
RR6-R9    VKGRFTISRDNAKKTVYLEMNSLEPEDTAVYYCYTHYFR-------------------SYWGQGTQVTVSS
RR6-R2    VKGRFTISRDNAKTTVYLQMNSLKPEDTAVYYCAARPVRVDDISLPVGF--------DYWGQGTQVTVSS
RR1-52    VKGRFAVSRDNAKNTVNLQMNSLKPEDTAVYYCAAKTTTWGGNDPNNW---------NYWGQGTQVTVSS
hCG-H14   VRGRFTISRDNAKKTVYLQMNSLKPEDTAVYTCGAGEGGTW----------------DSWGQGTQVTVSS
cAb-Lys3  VKGRFTISQDNAKNTVYLLMNSLEPEDTAIYYCAADSTIYASYYECGHGLSTGGYGYDSWGQGTQVTVSS
cAb-RN05  VKGRFTISRDKGKNTVYLQMDSLKPEDTATYYCAAGGYELRDRTY------------GQWGQGTQVTVSS
cAb-CA05  VKGRFTISQDNAKNTVYLQMNSLKPEDTAIYYCAGSTVASTGWCSRLRPYDY-----HYRGQGTQVTVSS
AMYL-B07  VKGRFTISRDNAKNTAYLQMDSLKPEDTAVYYCAAGPGSGKLVVAGRTCYGP-----NYWGQGTQVTVSS
AMYL-D09  VKGRFTLSQDNNKNTVYLQMNSLKPEDTGIYYCATGNSVRLASWEGY----------FYWGQGTQVTVSS
AMYL-D10  VKGRFTISQGNAKNTAYLQMDSLKPDDTAMYYCKPSLRYGLPGCPI-----------IPWGQGTQVTVSS
```

Fig. 1. Alignment of 10 sequences of camelid VHHs with known structures. From top to bottom: RR6-R9: llama VHH number 9 (raised against red dye RR6, this work); RR6-R2: llama VHH number 2 (raised against red dye RR6, PDB entry 1QD0 [12]); RR1-52: llama VHH number 52 (raised against red dye RR1, PDB entry 1I3V/1I38 [13]); hCG-H14: llama VHH number H14 (raised against hCG, PDB entry 1HCV [6]); cAb-LY3: camel VHH anti-lysozyme 3 (raised against lysozyme, PDB entry 1MEL [8]); cAb-RN05: camel VHH anti-RNase-5 (raised against RNAse, PDB entry 1B2Q [9]); cAb-CA05: camel VHH anti-carbonic anhydrase 5 (raised against carbonic anhydrase, PDB entry 1GGV [10]); AMYL-B07, -D09 and -D10: camel VHHs anti-amylase number B07, D09, D10 (raised against porcine amylase, PDB entries 1KXT, 1KXQ and 1KXV [11]). The CDR residues are colored red, green and blue for CDRs 1, 2 and 3, respectively. Cysteines are colored yellow. Residues characteristic of camelid VHHs are colored pink. Numbering is that of Kabat et al. [37].

Table 2
Affinity values of several llama VHHs for their antigen, the red dye RR6

Llama VHH	K_d (nM)
R2	22
R7	45
R8	20
R9	83
R10	58

3. Results

3.1. Characteristics of the anti-RR6 VHH-R9 sequence

The VHH-R9 fragment sequence is closely related to that of the other VHH fragments from camel or llama of known 3D structure (Fig. 1). It displays the four amino acid mutations observed in all camelid VHHs as compared to classical VHs: Val37Tyr (instead of Phe in most VHHs), Gly44Gln (instead of Glu), Leu45Arg and Trp47Leu, the latter position being sometimes substituted by Gly, Tyr, Phe and Ser in other VHHs. VHH-R9 possesses two cysteines (Cys22 and Cys92) forming the conserved disulfide bridge present in all VH and VHH domains. The CDR1 is nine residues long, a length typical of most VHHs [14], and its CDR2 is seven residues long, a value observed in many camelid VHH (Fig. 1). In contrast, the CDR3 is only six residues long, a value largely below the average size of CDR3 in camels or llamas (Fig. 1). Very short CDR3s have been reported for classical antibodies, though, such as that belonging to an immunoglobulin raised against ampicillin [25]. However, VHH-R9 possesses the shortest CDR3 observed in camels or llama antibodies, to date.

3.2. Characterization of the VHH-R9

The affinity of the VHH-R9 for RR6 has been measured on an IAsys biosensor (Table 2). Its K_d value, measured on freshly purified protein, was 83 nM, a value slightly higher than but within the same order of magnitude as those observed with other RR6 hapten binders (values between 22 and 58 nM, Table 2).

Matrix-assisted laser desorption/ionization mass spectroscopy performed on freshly purified protein yielded a single peak at 12 610 Da, accounting for the intact VHH with pyroglutamine at position 1. The mass spectra performed on samples of proteins remaining from crystallization experiments contain several peaks. The main peak belongs to the intact native VHH-R9 (MW = 12 610). The three different peaks with lower intensity at 12 028 Da, 11 899 Da and 11 813 Da were attributed to VHH-R9 missing the first five, six and seven amino acids at the N-terminus, respectively. Peaks corresponding to VHH-R9 dimers have also been observed, but at lower intensity. The low intensity of the dimers in the mass spectrum could be due to the acidic conditions of the experiment, since sinapinic acid is the matrix used in these measurements.

3.3. The VHH-R9 structure and the domain swapped dimer

The complete VHH-R9 sequence consists of 114 amino acids, numbered 1–113 (Fig. 1). Molecular replacement was performed using as a starting model the core residues (CDRs were excluded) of VHH-R2 (PDB entry 1QD0 [12]). As mentioned above, the first seven amino acids were not visible in the electron density map, due to cleavage (see above). Residue 8 is a glycine forming a bulge between two stranded segments and is very exposed to solvent in VHH structures, hence its susceptibility to cleavage. The stretch of residues $S_{25}GNT_{28}$, at the beginning of CDR1, could not be traced due to weak

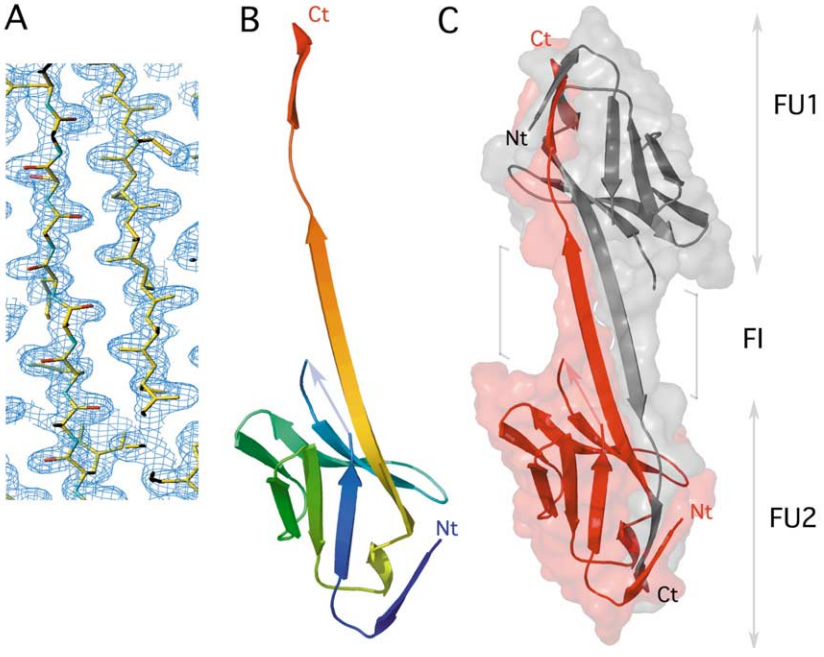

Fig. 2. Structure of VHH-R9. A: Electron density map ($2F_o-F_c$) displaying the two extended β-strand stretches of residues Tyr93–Trp103 in monomers A and B, forming the junction between the domain-swapped domains. The two stretches form an antiparallel β-structure well defined in density. B: Ribbon representation of VHH-R9 monomer in rainbow coloring. The blue arrow between strands 2 and 3 indicates the connectivity of CDR1, since a gap of four residues is present. C: The dimer reconstituted by associating the molecule in the asymmetric unit (red) with the closest symmetry-related molecule (gray). The two functional units (FU) are labelled FU1 and FU2, and the free interface, FI. The molecular surfaces are displayed in a semi-transparent fashion. View A was made with Turbo-Frodo [21], views B and C with PyMol [38].

electron density. Contrary to the former case, this is due to disorder since mass spectroscopy indicates the presence of these residues. We encountered some difficulties when trying to trace the CDR3. It became rapidly obvious that it was impossible to model a loop, but that a long stretch of residues was extending beyond the VHH molecular boundary, first in the solvent, and then along a symmetry-related molecule (Fig. 2A,B). When crystal symmetry was applied, it became obvious that VHH-R9 was displaying a domain-swapped structure [15,26,27]: the last β-strand of each symmetry-related domain was provided by its closest neighbor (Fig. 2C). The two symmetry-related molecules form a strongly bound anti-parallel structure resembling a dumb-bell. Considered as a whole, the incomplete VHH monomer and the last β-strand from the other monomer reconstitute a classical VHH (not considering the CDR3), superimposable on other VHH structures. This composite structure is called a functional unit (FU) in the domain-swapping nomenclature [15], and the domain-swapped elements between the two FUs are called free interface (FI). It should be noticed, however, that in the case of VHH-R9, the FU is no longer functional due to the destruction of the combining site. When superimposing the VHH-R9 FU with, e.g. VHH-52, all structural elements are well aligned (rmsd of 1.04 Å on 94 amino acids kept in the alignment) (Fig. 3A). The intricacy of the association in the crystal suggests, as for other domain-swapped dimers, that it pre-exists in solution. This is most likely true since the monomer surface buried in the interaction is 1660 Å^2, on a total surface of 7680 Å^2. It accounts for 21% of the molecular surface, when values above 8% have been shown to be relevant of biologically relevant dimers [28]. Furthermore, the observation of a dimer in harsh mass spectroscopy conditions reveals the strength of the interaction. Such domain-swapped dimers have already been observed by mass spectroscopy in similar conditions [27].

The driving force for the CDR3 opening and the projection of the ninth strand outwards is probably twofold: first, the short CDR3 should impose some strain on the VHH backbone; second, the depletion of residues 1–7 probably weakens the interaction between the ninth strand and the rest of the VHH. In VH or VHH domains, the N- and C-terminal closure involves interactions of strands 1a and 2, 1b and 9b, and 9b with 8 (Fig. 3B). This alternate pattern of interactions of strand 1 ensures proper closure of the β-sandwich (Fig. 3B). The lack of strand 1a weakens strand 9 position since: (i) indirect interactions are normally established between strands 1a and 9b through water molecules; (ii) the lack of strand 1a

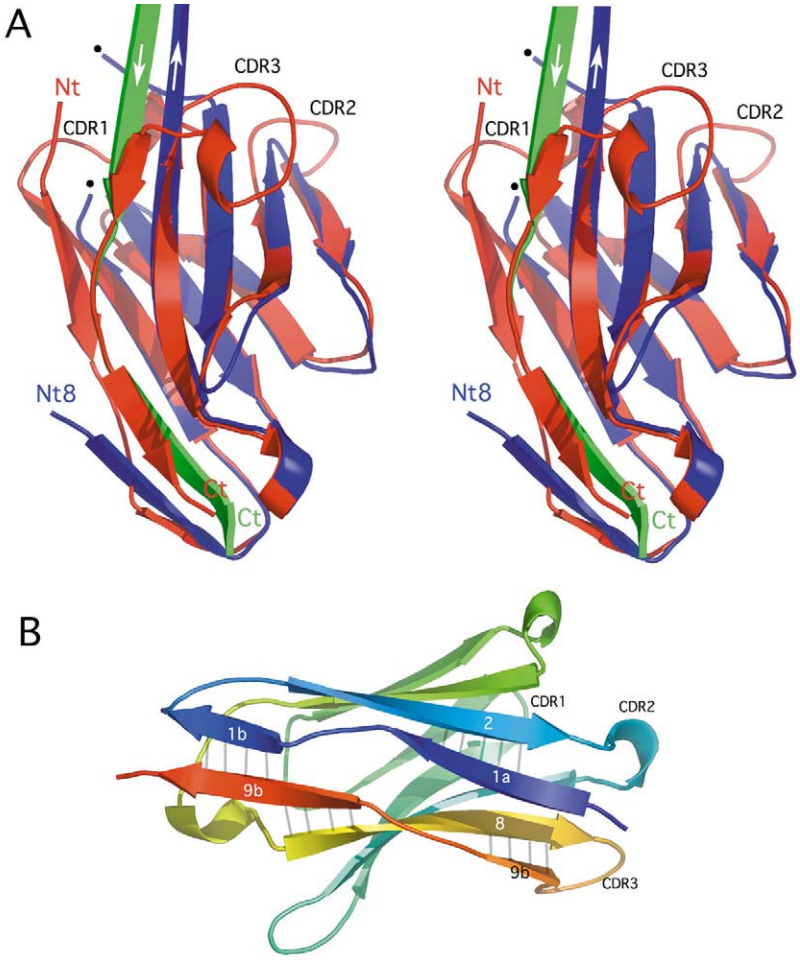

Fig. 3. Mechanism of domain swapping. A: The FU of VHH-R9 (blue and green) superimposed with VHH-RR1-52 (red). The CDRs are identified. For VHH-R9, the gap in CDR1 is localized by two black dots; CDR3 is replaced by the swapped segments, and β-strand 1 is shorter and displaced outwards. The rest of the molecule superimposes well with VHH-RR1-52. B: Rainbow ribbon representation of a camelid VHH displaying the closure mechanism. The β-strands are labelled 1–9, and the CDRs are identified. The interactions between the strands involved in domain closing are symbolized by thick gray lines. Views made with PyMol [38].

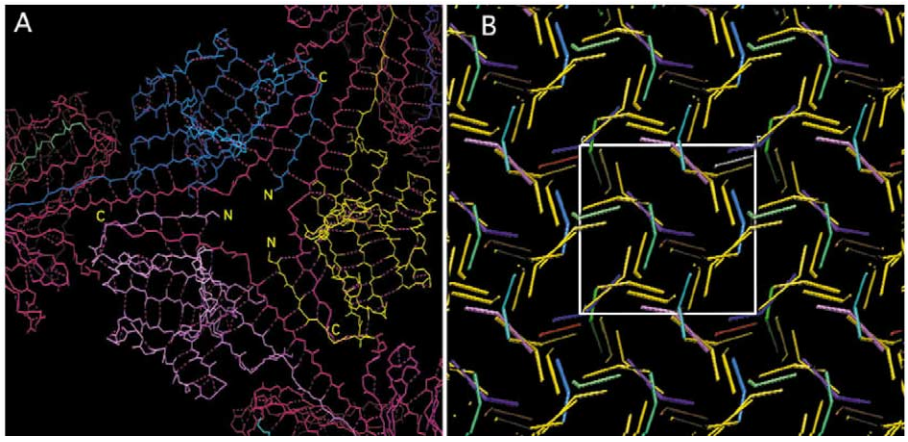

Fig. 4. Representation of the crystal packing of VHH-R9. A: View of the peptide backbone along the threefold axis; the N- and C-termini are identified and the main chain hydrogen bonds are displayed. B: View of the cubic crystal packing ($I4_132$) parallel to a plane. A unit cell is displayed as a white square. For clarity, only residues in segment 90–113 have been displayed schematically as a broken line. Views made with Turbo-Frodo [21].

weakens strand 1b which assumes a more open position in VHH-R9 and does not interact correctly with 9b. At that stage, the strain induced by CDR3 might provoke the opening of strand 9. Once this strain is released, conditions are restored for establishing favorable connections between the domain-swapped strand 9 and another open VHH-R9. The association then remains stable, since the strain exerted by the short CDR3 is no longer present.

3.4. Formation of larger β-stranded structures

Besides the dimer association, the dimers establish a large network of interactions in the crystal. It is formed of trigonal structures involving the N- and C-terminal segments arranged around the cubic threefold axis (Fig. 4A). Noteworthy, these contacts could not be established if the N-terminus was left intact. This ternary motif involves six VHH molecules linked by a dense and large network of inter-strand hydrogen bonds (Fig. 4A). This motif is ramified in other identical motifs, rotated by 90°. They all form a continuous β-stranded structure spanning in three dimensions along the whole crystal assembly (Fig. 4B).

4. Discussion

Crystals of immunoglobulin domains have been described as a potential source of pathologies due to abnormal physiological behavior. As an example, accumulation of non-covalent immunoglobulin κ light chain dimers (Bence–Jones protein) leads to renal complications, such as the Fanconi syndrome, a specific proximal tubule impairment [29]. In this case as in other cases, however, accumulation of non-swapped VL–VL dimers is observed, leading to micro-crystals in the renal tubules. The only case of domain swapping reported in immunoglobulins is the exchange of the VL and VH domains in Fvs, a process used in biotechnology to provide multiple specificities to dimeric (or multimeric) Fvs [30]. Once again, the immunoglobulin domains themselves (VL and VH) have been shown to be intact in a natively folded state.

It has been reported that residues at the N-terminus of VH domains are conformationally important, as illustrated in an anti-ampicillin Fv domain [25,31]. Mutations introduced at positions 6 and 10 induced a drastic conformational change of the first nine residues, which were no longer in contact with the core of the VH, but established a serendipitous contact with a symmetry-related molecule. In VHH-R9, however, the first strand sequence, up to residue 15, is identical to those of other VHHs (Fig. 1). The cleavage at positions 5–7 should therefore be due to a proteolytic process occurring during the long time of crystallization.

Dimerization by domain swapping has been reported to have a high activation energy (slow kinetics) because of drastic conformational changes, associated with a small thermodynamic driving force, due to the similarity between the initial and final structures [15,32]. Since no direct interface is observed between the VHH FUs in the dimer and since the VHH fold is conserved, the CDR3 strain release and the interactions in the hinge extension should account for most of the favorable energy changes. The length of the hinge has been shown to play a crucial role in the case of the domain-swapped bovine odorant binding protein (bOBP). Compared to other OBPs, bOBP is devoid of disulfide bridges and possesses a shorter turn, lacking a Gly residue, between its β-barrel and its last α-helix [26]. As a consequence, helices are exchanged between two molecules resulting in a C-terminal domain-swapped dimer. By inserting a Gly residue after position 121, a monomeric bOBP could be obtained [27], hence confirming the essentiality of the hinge in the phenomenon. Although not tested in the case of VHH-R9, we postulate that the hinge size (the CDR3) is pivotal to yield domain swapping in this case also.

Another favorable energy source might be the energy of dimer association in the crystal. The strong hydrogen bonds established between strands in dimers and between dimers should account for a large proportion of the energy gained upon swapping. The high concentration conditions used in crystallization should displace the equilibrium towards the dimer and, further, towards larger polymers possibly preformed along the crystallization route. Lastly, the formation of crystals should also displace the equilibrium to the dimers by removing them from the soluble phase (mass action law).

Extended networks of interactions are observed in amyloid fibers, which are also the result of an initial domain-swapping step [15,32–36]. Human cystatin C, a protein which reveals amyloidic properties through a L68Q mutation, exists as a

monomer or a domain-swapped dimer. Two monomers exchange two of their β-strands (plus an α-helix) creating a long anti-parallel double-stranded free interface [35], resulting in the same dumb-bell topology as VHH-R9. This dimer, however, unlike VHH-RR9, exhibits classical crystal packing contacts, based on van der Waals contacts and few hydrogen bonds.

5. Conclusion

The crystal structure of VHH-R9 exhibits a domain-swapping pattern unique in the immunoglobulin field, to date. The crystal packing contacts are established through an extended 3D network of main chain strand–strand associations between different dimers. Since VHH-R9 has been shown to be functional in solution, having a low K_d against the hapten, it is likely that during the time of the crystallization process (4–5 weeks) elements such as N-terminal cleavage, high concentration conditions and short CDR3, lead to the domain-swapping and condensation phenomena.

Acknowledgements: The ESRF is greatly acknowledged for beam time allocation. This study was supported in part by the EU BIOTECH Structural Biology project (BIO4-98-048), by the CNRS and by the PACA region.

References

[1] Padlan, E.A. (1994) Mol. Immunol. 31, 169–217.
[2] Hamers-Casterman, C., Atarhouch, T., Muyldermans, S., Robinson, G., Hamers, C., Songa, E.B., Bendahman, N. and Hamers, R. (1993) Nature 363, 446–448.
[3] Nguyen, V.K., Hamers, R., Wyns, L. and Muyldermans, S. (1999) Mol. Immunol. 36, 515–524.
[4] Woolven, B.P., Frenken, L.G., van der Logt, P. and Nicholls, P.J. (1999) Immunogenetics 50, 98–101.
[5] Muyldermans, S., Atarhouch, T., Saldanha, J., Barbosa, J.A. and Hamers, R. (1994) Protein Eng. 7, 1129–1135.
[6] Spinelli, S., Frenken, L., Bourgeois, D., de Ron, L., Bos, W., Verrips, T., Anguille, C., Cambillau, C. and Tegoni, M. (1996) Nat. Struct. Biol. 3, 752–756.
[7] Dolk, E., van der Vaart, M., Hulsik, D.L., Vriend, G., Spinelli, S., Cambillau, C., Frenken, L. and Verrips, T., Appl. Environ. Microbiol. (submitted).
[8] Desmyter, A., Transue, T.R., Ghahroudi, M.A., Dao Thi, M.H., Poortmans, F., Hamers, R., Muyldermans, S. and Wyns, L. (1996) Nat. Struct. Biol. 3, 803–811.
[9] Decanniere, K., Desmyter, A., Lauwereys, M., Ghahroudi, M.A., Muyldermans, S. and Wyns, L. (1999) Structure 7, 361–370.
[10] Desmyter, A., Decanniere, K., Muyldermans, S. and Wyns, L. (2001) J. Biol. Chem. 276, 26285–26290.
[11] Desmyter, A., Spinelli, S., Lauwereys, M., Wyns, L., Muyldermans, S. and Cambillau, C. (2002) J. Biol. Chem. 277, 23645–23650.
[12] Spinelli, S., Frenken, L.G., Hermans, P., Verrips, T., Brown, K., Tegoni, M. and Cambillau, C. (2000) Biochemistry 39, 1217–2122.
[13] Spinelli, S., Tegoni, M., Frenken, L., van Vliet, C. and Cambillau, C. (2001) J. Mol. Biol. 311, 123–129.
[14] Muyldermans, S., Cambillau, C. and Wyns, L. (2001) Trends Biochem. Sci. 26, 230–235.
[15] Liu, Y. and Eisenberg, D. (2002) Protein Sci. 11, 1285–1299.
[16] Frenken, L.G., van der Linden, R.H., Hermans, P.W., Bos, J.W., Ruuls, R.C., de Geus, B. and Verrips, C.T. (2000) J. Biotechnol. 78, 11–21.
[17] Matthews, B.W. (1968) J. Mol. Biol. 33, 491–497.
[18] Otwinovski, Z. (1993) in: Data Collection and Processing (Sawyer, L., Isaacs, N.W. and Bailey, S., Eds.), pp. 56–63, DLSCI/R34 Daresbury Laboratory, Daresbury.
[19] CCP4, Collaborative Computational Project No. 4 (1994) Acta Crystallogr. D 50, 760–763.
[20] Navaza, J. (1990) Acta Crystallogr. A 46, 619–620.
[21] Roussel, A. and Cambillau, C. (1991) in: Silicon Graphics Geometry Partners Directory, Vol. 81, Silicon Graphics, Mountain View, CA.
[22] Brunger, A.T., Adams, P.D., Clore, G.M., DeLane, W.L., Gros, P., Grosse-Kustleve, R.W., Jiang, J.S., Kuszewski, J., Nilges, M., Panun, N.S., Read, R.J., Rice, L.M., Simonson, T. and Warren, G.L. (1998) Acta Crystallogr. D 54, 905–921.
[23] Murshudov, G.N., Vagin, A.A. and Dodson, E.J. (1997) Acta Crystallogr. A 50, 157–163.
[24] Laskowski, R.A., MacArthur, M.W., Moss, D.S. and Thornton, J.M. (1993) J. Appl. Crystallogr. 26, 283–291.
[25] Burmester, J., Spinelli, S., Pugliese, L., Krebber, A., Honegger, A., Jung, S., Schimmele, B., Cambillau, C. and Plückthun, A. (2001) J. Mol. Biol. 309, 681–695.
[26] Tegoni, M., Ramoni, R., Bignetti, E., Spinelli, S. and Cambillau, C. (1996) Nat. Struct. Biol. 3, 863–867.
[27] Ramoni, R., Vincent, F., Accornero, P., Valencia, C., Ashcroft, A.E., Grolli, S., Tegoni, M. and Cambillau, C. (2002) Biochem. J. 365, 739–748.
[28] Janin, J. and Rodier, F. (1995) Proteins 4, 580–587.
[29] Roussel, A., Spinelli, S., Déret, S., Navaza, G., Aucouturier, P. and Cambillau, C. (1999) Eur. J. Biochem. 260, 192–199.
[30] Arndt, K.M., Muller, K.M. and Pluckthun, A. (1998) Biochemistry 37, 12918–12926.
[31] Jung, S., Spinelli, S., Schimmele, B., Honegger, A., Pugliese, A., Cambillau, C. and Plückthun, A. (2001) J. Mol. Biol. 309, 701–716.
[32] Staniforth, R.A., Giannini, S., Higgins, L.D., Coroy, J.M., Hounslow, A.M., Jerala, R., Craven, J.C. and Waltho, J.P. (2001) EMBO J. 20, 4774–4781.
[33] Rousseau, F., Schymkowitz, J.W.H. and Wilkinson, H.R. (2001) Proc. Natl. Acad. Sci. USA 98, 5596–5601.
[34] Liu, Y., Gotte, G., Libonati, M. and Eisenberg, D. (2001) Nat. Struct. Biol. 8, 211–214.
[35] Janowski, R., Kozak, M., Jankowska, E., Grzonka, Z., Grubb, A., Abrahamson, M. and Jaskolski, M. (2001) Nat. Struct. Biol. 8, 316–320.
[36] Knaus, K.J., Morillas, M., Swietnicki, W., Malone, M., Surewicz, W.K. and Yeel, V.C. (2001) Nat. Struct. Biol. 8, 770–774.
[37] Kabat, E., Wu, T.T., Perry, H.M., Gottesman, K.S., Foeller, C. (1991) Publication No. 91-3242, US Public Health Services, NIH, Bethesda, MD.
[38] DeLano, W.L., The PyMOL Molecular Graphics System. DeLano Scientific LLC, San Carlos, CA (http://www.pymol.org).